Sensors and Actuators B 228 (2016) 295–301

Contents lists available at ScienceDirect

Sensors and Actuators B: Chemical

journal homepage: www.elsevier.com/locate/snb

Facile synthesis of In_2O_3 nanospheres with excellent sensitivity to trace explosive nitro-compounds

Yang-Yang He, Xu Zhao, Yang Cao, Xiao-xin Zou, Guo-Dong Li*

State Key Laboratory of Inorganic Synthesis and Preparative Chemistry, International Joint Research Laboratory of Nano-Micro Architecture Chemistry, College of Chemistry, Jilin University, 2699 Qianjin Street, Changchun 130012, China

ARTICLE INFO

Article history:
Received 24 September 2015
Received in revised form 9 January 2016
Accepted 12 January 2016
Available online 15 January 2016

Keywords:
In_2O_3
Explosives
Gas sensor
Nanospheres
Nitrocompounds

ABSTRACT

In_2O_3 nanospheres with excellent sensing ability to explosive nitro-compounds have been successfully synthesized via a two-step method including a mild solvothermal process and calcination at elevated temperature in air. The as-synthesized In_2O_3 nanospheres are of 200–300 nm in diameter and are composed of small nanoparticles with a size of around 5 nm. The structure, morphology and thermal stability are investigated by XRD, SEM, TEM, HRTEM, TG and XPS. At 140 °C, the responses of this sensor toward 100 ppm nitromethane, nitroethane and nitropropane are 163, 220 and 375, respectively. And what's more, the sensor also exhibits short response time of less than 1 s, good long-term stability, and low detection limits. The good sensing performance should be attributed to the strong electron-withdrawing effect of nitro group and low working temperature.

© 2016 Elsevier B.V. All rights reserved.

1. Introduction

In recent years, the research interest in the detection of nitro-containing compounds, both Nitroaromatic and Nitroalkane, has increased greatly due to their highly explosive and toxic nature [1]. They can usually cause heavy headaches, sore throat, abdominal pain, cancer and even lead to death at a low concentration [2]. Nitroaromatics, including 2, 4-dinitrotoluene (2, 4-DNT), 2, 6-dinitrotoluene (2, 6-DNT), 2, 4, 6-trinitrotoluene (TNT) and picric acid (PA) etc., are widely used in the fields of synthesizing pesticides, explosive, dye and textile industries. Nitroalkanes, involving nitromethane, nitroethane, nitropropane and 2, 3-dimetheyl-2, 3-dinitrobutane etc., are important pharmaceutical intermediates, regents for explosive and excellent solvents for vinyls, polyamides, epoxies and acrylic polymers, and so on [3]. Moreover, nitromethane can be used as rocket fuel. For the safety concern, it is necessary to detect these nitro-containing compounds mentioned above at a low concentration. Thus, many methods have been developed for the monitor of nitro-containing compounds, including ion mobility spectrometry [4], fluorescence spectrophotometry [5], mass spectrometry [6] and electrochemical sensor [7]. Although some of these methods can give high response, good selectivity and accuracy, they are expensive, high energy consumption and not portable. Furthermore, most of the above methods are complicated and require professional experts to operate the equipment and analyze the data. Obviously, it is important to develop low cost, convenient and portable gas sensors to detect those nitro-containing explosives for practical application.

Metal oxide semiconductor (MOS) with different compositions and structures, including SnO_2, ZnO, In_2O_3, TiO_2 and Fe_2O_3 etc., have been widely investigated for reductive and oxidative gas detecting [8]. Among those MOS, In_2O_3, an important n-type semiconductor with a wide band gap of 3.6 eV and good conductivity, has been extensively studied in the area of solar cell, display, gas sensor, photocatalysis and so on [9–12]. Up to now, In_2O_3 materials with different structures and morphologies have been prepared, such as nanowires, nanorods, nanoparticles, nanocubes, nanofibers, nanoplates and nanospheres [11–17]. They showed excellent sensing ability to acetone, carbon monoxide, chlorine, ethanol, hydrogen sulfide, ammonia and/or other volatile organic compounds (VOCs) [18–31]. However, none of them was related to the detection of trace explosive nitrocompounds in air.

Herein, we report an In_2O_3 nanospheres based sensor with excellent sensing performance to the above nitroalkane at relatively low operating temperature of 140 °C. To verify the action of nitro group during the sensing process, methane, ethane and propane were also investigated. For the strong electron-withdrawing effect of nitro group, nitroalkane can be activated

* Corresponding author. Fax: +86 43185168624.
E-mail addresses: lgd@jlu.edu.cn, lifind@21cn.com (G.-D. Li).

http://dx.doi.org/10.1016/j.snb.2016.01.042
0925-4005/© 2016 Elsevier B.V. All rights reserved.

Scheme 1. The schematic graphs of nitromethane, nitroethane and nitropropane.

(Scheme. 1) and react with oxygen species adsorbed on the surface of In_2O_3 at 140 °C, whereas, alkane such as methane, ethane and propane is inactive at this condition. Thus, we believe that it would promote the development of detecting nitro-explosive at low concentration levels.

2. Experimental

2.1. Synthesis of In_2O_3 nanospheres

Firstly, indium alkoxide nanospheres were synthesized via a solvothermal process by using the mixture of ethanol, ethylene glycol and 1, 3-propanediol. Secondly, the final In_2O_3 nanospheres were obtained by calcining the indium alkoxide precursor at elevated temperature in air. 1, 3-propanediol was purchased from Shanghai Demand Chemical Co., Indium (III) nitrate hydrate was purchased from Sinopharm Chemical Reagent Co., Ltd. Ethylene glycol and ethanol were purchased from Beijing Chemical Works. All the reagents and chemicals used in our experiments are analytical grade and without further purification. In a typical synthetic procedure, $In(NO_3)_3{\cdot}4.5H_2O$ (0.30 g) was added into a mixture of ethanol (30 mL), ethylene glycol (5 mL) and 1, 3-propanediol (5 mL) and stirred till the formation of homogeneous colorless and transparent solution. Then, the solution was transferred into a 100 mL Teflon-lined autoclave and heated at 180 °C for 6 h. The obtained white indium alkoxide solid product was separated from the solution by centrifugation, then washed with absolute ethanol, and dried at 80 °C in air. The In_2O_3 nanospheres were prepared by the subsequent calcination of indium alkoxide at 300 °C, 400 °C, 500 °C in air for 2 h and the related products were denoted as S300, S400, S500, respectively.

2.2. Structural characterization

The X-ray powder diffraction (XRD) patterns were obtained on a Rigaku D/Max 2550 X-ray diffractometer using Cu Kα radiation (λ = 1.5418 Å) operated at 200 mA and 50 kV. The scanning electron microscopic (SEM) images were taken on a JEOL JSM 6700F electron microscope, while the transmission electron microscopy (TEM) images were recorded with a Philips-FEI Tecnai G2S-Twin. The X-ray photoelectron spectroscopy (XPS) was measured on an ESCALAB 250 X-ray photoelectron spectrometer with a monochromatic X-ray source (Al Kα hυ = 1486.6 eV). The thermal gravimetric analysis (TG) curve for the precursor was conducted in air on a NETZSCH STA 449C TG thermal analyzer from 25 to 800 °C at a heating rate of 10 °C min^{-1}.

2.3. Sensor fabrication and response testing

To assemble sensors, In_2O_3 nanospheres were dispersed in an appropriate amount of ethanol to form viscous slurry by milling. The gas sensor was fabricated by coating the slurry on the surface of a ceramic tube with a tiny brush. The length and diameter of this tube are 4 mm and 1 mm, respectively. And there are two gold electrodes and four platinum wires on both ends of the ceramic tube. A Nickel-chromium alloy coil was inserted into the tube and was used as a heating unit for tuning the operating temperature of the sensors (Scheme. 2). After ageing at 200 °C for 12 h, the sensing properties of the In_2O_3 sensor were tested on a commercial CGS-8 gas sensing measurement system (Beijing Elite Tech Company Limited) with a static gas sensing chamber. The sensor response value is depicted as the ratio of Ra/Rg, where Ra is the resistance in fresh air, Rg is the resistance in the desired concentration of target gas diluted with fresh air. Response and recovery time is defined as

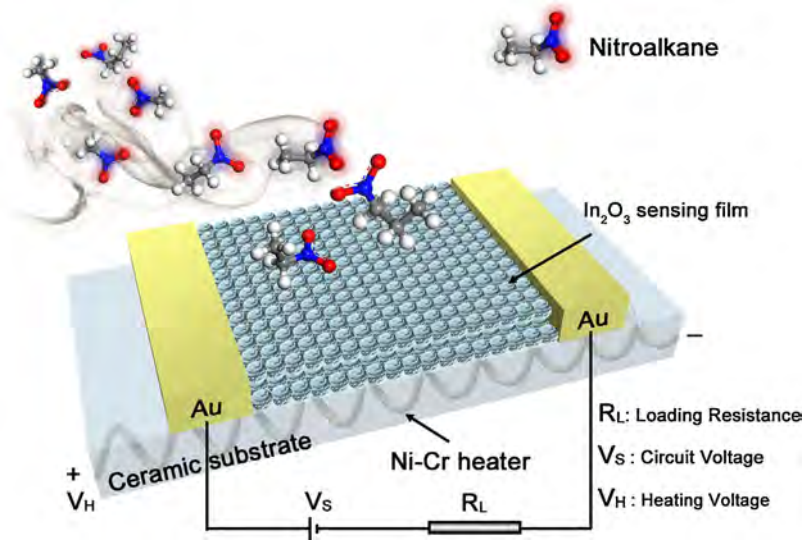

Scheme 2. Schematic illustration of the sensor's structure.

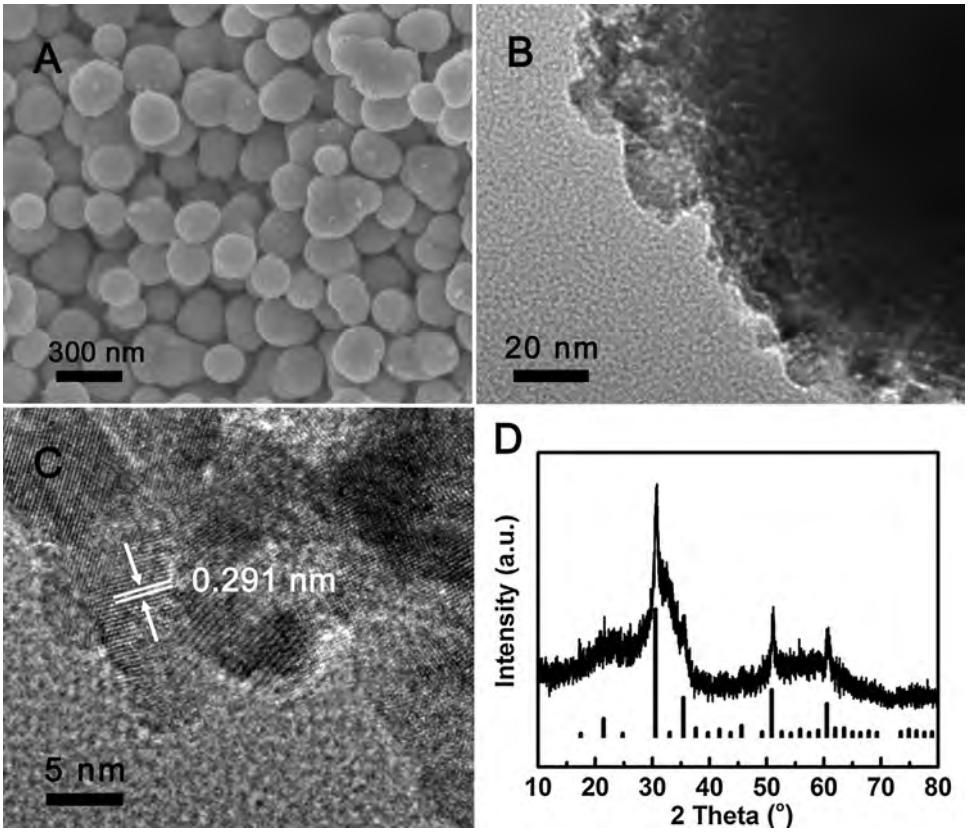

Fig. 1. (A) SEM image, (B) TEM and (C) HRTEM image and (D) XRD pattern of S300.

the time taken by the sensor to achieve 90% of the total resistance change in the process of adsorption and desorption, respectively.

3. Results and discussion

A typical SEM image of S300 was shown in Fig. 1A. The S300 is nearly the same as that of as synthesized indium alkoxide precursor (Fig. S1A) except the slightly shrink in size due to the removal of organic species in the spheres. To understand the structure of the indium oxide, TEM images and XRD pattern were obtained (Fig. S1B–D). The TEM and HRTEM images of S300 (Fig. 1B and C) indicate that these In_2O_3 nanospheres are composed of tiny nanoparticles with a size of around 5 nm. And the rough surface of In_2O_3 nanospheres (Fig. 1A and B) can be attributed to the in situ assembly of small nanoparticles into nanospheres [32]. The SEM images of the In_2O_3 nanospheres calcined at various temperatures are shown in Fig. S2. It is clear that the size of the obtained In_2O_3 nanospheres shrink a little due to the loss of organic species in the precursor.

In order to confirm the structure of the product, High-resolution TEM image of In_2O_3 nanospheres was obtained as shown in Fig. 1C. The fringe spacing of 0.291 nm can be identified as the (2 2 2) crystal

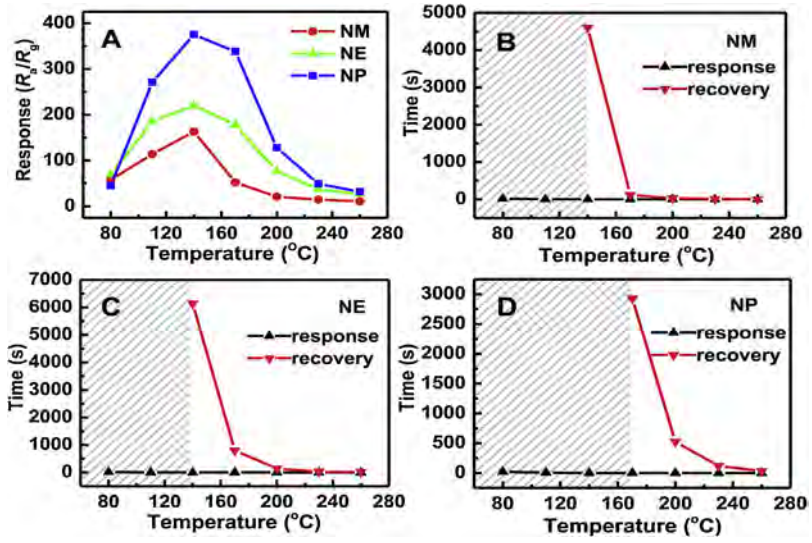

Fig. 2. (A) Response and (B), (C), (D) response and recovery time versus operating temperature to NM, NE and NP for S300.

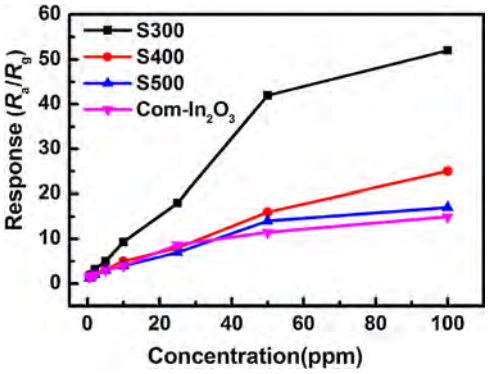

Fig. 3. The response versus various concentrations of nitromethane for S300, S400, S500 and commercial In_2O_3 sensor.

planes of cubic In_2O_3. In Fig. 1D, the XRD pattern of the product is also in accordance with a cubic In_2O_3 (JCPDS card No. 65–3170). The XRD patterns of S300, S400 and S500 were shown in Fig. S3. With the increase of the heating temperature, the XRD peaks of the products become sharp indicating the crystal size and crystallinity of the products gradually increased.

To investigate the thermal stability of indium alkoxide precursor and determine the temperature for calcination, thermogravimetric analysis (TGA) was carried out in air from room temperature to 800 °C (Fig. S4). The weight loss can be assigned to the removal of the absorbed water (25–100 °C), the decomposition of organic component (100–300 °C) and the loss of hydroxyls (300–800 °C), respectively.

Metals which located in the d-, ds-, f-, and p-blocks of the periodic table can form solid-state metal alkoxides, such as Ti, Fe, Co, Ni, In, Sn and so on. And they will be formed metal oxide after calcination [33]. In this work, we use ethylene glycol and 1, 3-propanediol as the reagents. Ethylene glycol has been established as a cross-linking reagent and has been used for the synthesis of porous metal oxide [34]. During calcination, the organic species would be destroyed or burned and Indium would be turned into porous In_2O_3 composed of nanoparticles, which was reported elsewhere [35–37]. It should be a solid reaction without melting the

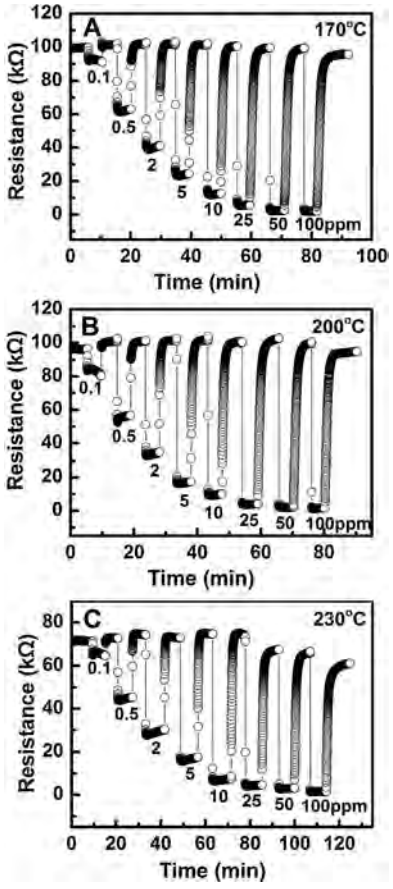

Fig. 4. The dynamic response-recovery features of the S300 sensor for 0.1-100 ppm (A) NM, (B) NE and (C) NP.

precursor due to the morphology and particle size of the product and the precursor was nearly the same. While the release of CO_2 and other gas favored the formation of porous In_2O_3 nanospheres.

The sensing performance of the sensor fabricated by S300 was investigated in detail. And we found that S300 gave excellent

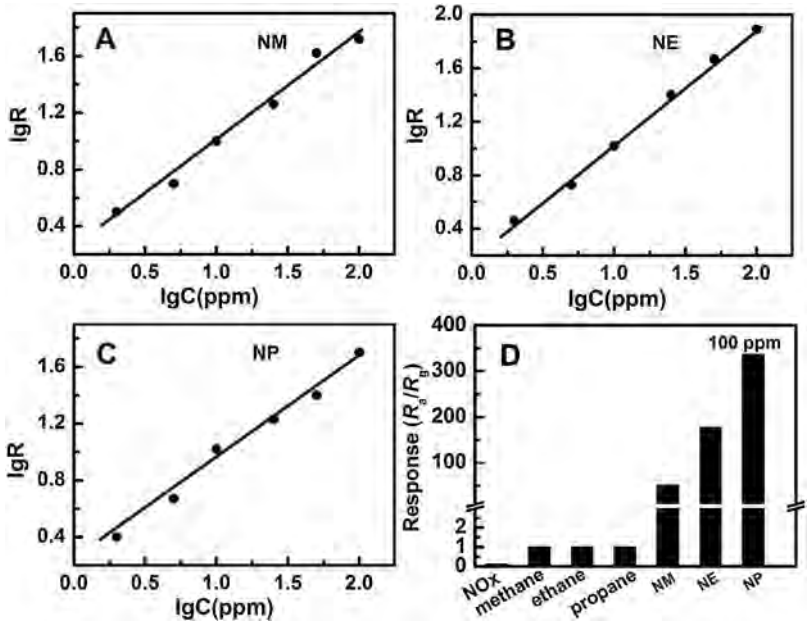

Fig. 5. The relation between response and the concentration of (A) NM, (B) NE and (C) NP, (D) responses of S300 sensor to 100 ppm different gases at 170 °C.

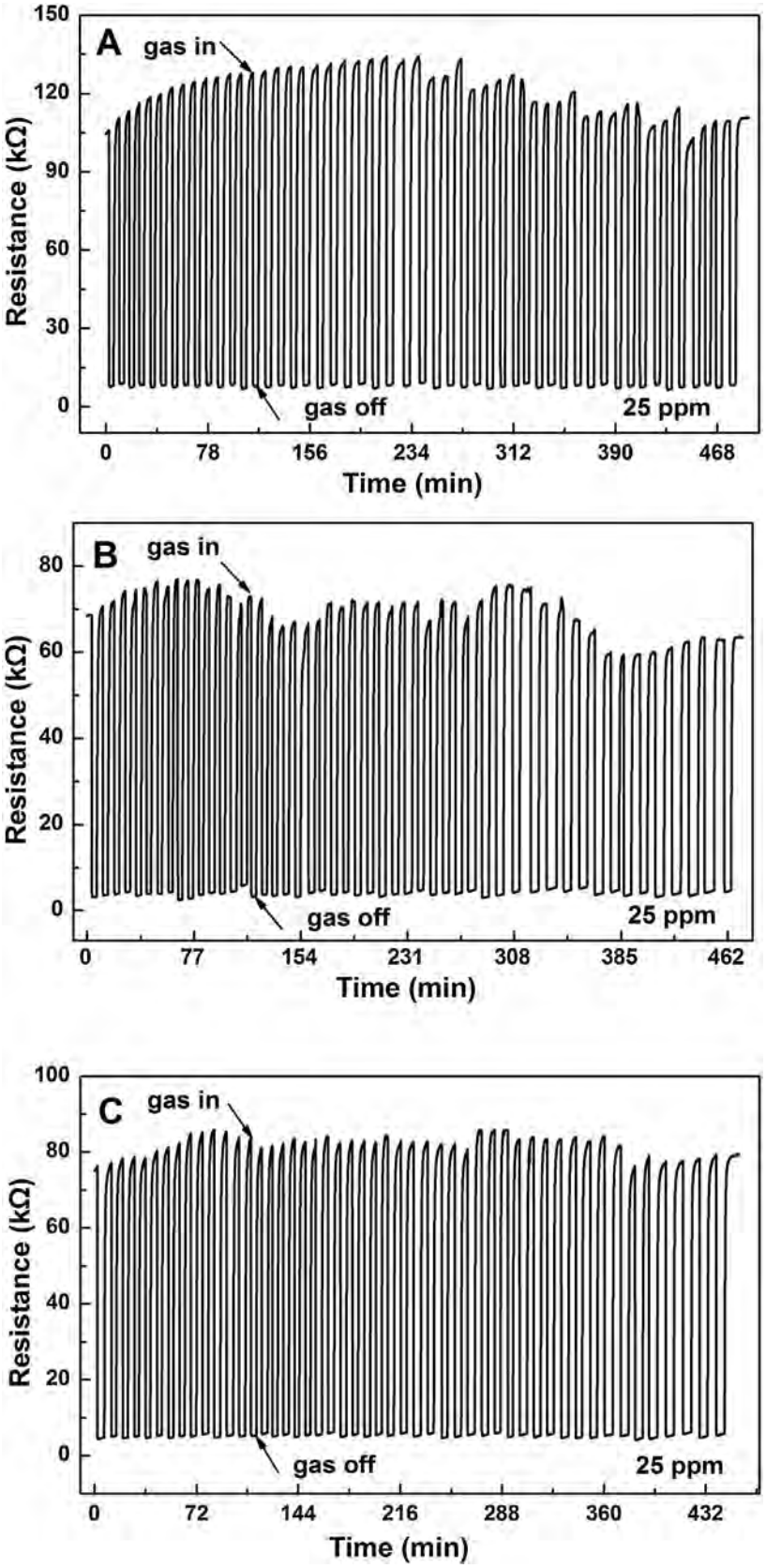

Fig. 6. The stability of S300 In_2O_3 sensor to (A) NM, (B) NE and (C) NP, respectively.

responses to these nitroalkanes. It is well known that the response of gas sensor is significantly influenced by the operating temperature. In order to determine the optimal operating temperature of the as-prepared In_2O_3 sensor for the detection of nitromethane, nitroethane and nitropropane, the responses to 100 ppm target gases versus operating temperature were obtained in the range of

80–260 °C. As shown in Fig. 2A, the responses of the as-prepared In_2O_3 sensor to these gases increase gradually (80–140 °C) and then decrease with further increase the operating temperature (140–260 °C). The highest responses of the sensor to the three target gases are all reached at 140 °C. While, the response time and recovery time is also the important parameter for sensors. As shown in Fig. 2B–D, the as-fabricated In_2O_3 sensor exhibits short response time to these 100 ppm nitroalkanes in the temperature range of 80–260 °C. And the recovery time was obviously shortened with the increase of working temperature, which was in accordance with previous reports [38–41]. In this case, the recovery times are 4599, 121, 29, 13 and 6 s to nitromethane at 140, 170, 200, 230 and 260 °C, respectively.

Fig. 3 demonstrates the relationship between the response and the concentration of nitromethane for the products and commercial In_2O_3 sensor at 170 °C. It is obvious that S300 sensor exhibits much higher response than that of S400, S500 and commercial In_2O_3 sensors. As shown in Fig. S3, it is clear that the crystallinity of S300 is poorer than that of S400 and S500. In fact, amorphous materials would accompany more defects than those well crystalline materials, resulting in more active sites and adsorbed oxygen species [42]. The oxygen peak centered at 530 eV can be attributed to the lattice oxygen in crystalline In_2O_3, while the peak located at 531.7 eV is due to the chemisorbed oxygen species (O^{2-}, O_2—, O—) and OH— [43]. While, the amount of chemisorbed oxygen is in the order of S300 (47%) > S400 (38%) > S500 (35%) (Fig. S5). And what's more, the sensing ability will be greatly affected by these chemisorbed oxygen species, other than the physical absorbed oxygen [44]. As a result, it is reasonable that S300 gives the highest response for its high surface area, more active sites (amorphous state) and heavy chemisorbed oxygen.

The representative dynamic response-recovery features of the S300 sensor to different concentrations of nitromethane, nitroethane and nitropropane are presented in Fig. 4. The resistance of the as-prepared In_2O_3 sensor immediately decreased to a minimum resistance when the sensor was exposed to the target gases, and increased to the original value when the sensor was put in fresh air. And the S300 sensor can give a log linear between concentration and response for all the three gases as shown in Fig. 5A–C.

In addition, selectivity of the gas sensor is also an essential parameter of semiconductor materials. Fig. 5D illustrates the selectivity of the as-prepared In_2O_3 sensor to nitrocompounds and other typical gases at 170 °C. This sensor shows high response to nitromethane, nitroethane and nitropropane, while it exhibits much low response to other gases, including nitrogen oxides, methane, ethane and propane. The high response toward nitroalkane should be attributed to the activation effect of nitro group (—NO_2). As we all know, —NO_2 is a kind of strong electron withdrawing group, which can further decrease the negative charge density of α-C as shown in Scheme 1, leading to higher activity of those α-H atoms on the positive charged α-C in nitroalkane than those in alkane. For example, the electronegativity of some groups is in the order H < —CH_3 < —C_2H_5 < —*n*—C_3H_7 < —NO_2 [45], leading to charge density of α-C in alkane is higher than that of in nitroalkane. It is clear that oxygen species chemisorbed on the surface of In_2O_3 would be easily reduced by those activated molecules at low working temperature [46]. While, more electrons would be extracted by nitrogen oxide at high working temperature [47]. Thus, the as-prepared In_2O_3 sensor shows low response to methane, ethane and propane at the same condition. Fig. S6 shows the transient resistance change of the S300 sensor to 100 ppm NOx at 170 °C. The resistance of the S300 sensor rapidly rose to the maximum value in 1 s when NOx was introduced, and then returns to the initial resistance value when exposed in fresh air again. However, the resistance dramatically decreased when the In_2O_3 sensor was exposed to 100 ppm nitroalkane in air. Hence, the enhanced response of the as-prepared In_2O_3 sensor should be attributed to the activation effect of nitro group (—NO_2), rather than the nitro group itself.

In order to investigate the stability of the S300 gas sensor, the dynamic transient responses to these three nitro compounds were repeated for fifty times (Fig. 6). The responses of the sensor varied in a reasonable range, indicating the excellent long-term stability and satisfied reliability of the S300 In_2O_3 sensor.

For In_2O_3 nanospheres, a typical n-type metal oxide semiconductor, the gas sensing mechanism can be attributed to the surface-controlled mode [48–50]. That is, the resistance of the n-type metal oxide semiconductor is related to the depletion layer of the surface. The thickness of depletion layer located on the surface of the sensor will change in different atmospheres, resulting in the resistance change of the sensors.

4. Conclusions

In_2O_3 nanospheres composed of nanoparticles with enhanced nitroalkane sensing performance were obtained via a precursor method. The sensor made of In_2O_3 nanospheres (S300) exhibits quick response, high response value, low detection limit and excellent long-term stability. The high sensing activity to nitroalkane can be assigned to the activation effect of nitro groups (—NO_2) and relatively low working temperature.

Acknowledgments

This work was supported by the NSFC (21371070, 21401066); Jilin province science and technology development projects (20150520003JH, 20140101041JC, 20130204001GX and 20130206056GX) and Key Laboratory of Functional Inorganic Material Chemistry (Heilongjiang University), Ministry of Education.

Appendix A. Supplementary data

Supplementary data associated with this article can be found, in the online version, at http://dx.doi.org/10.1016/j.snb.2016.01.042.

References

[1] P. Kolla, The application of analytical methods to the detection of hidden explosives and explosive devices, Angew. Chem. Int. Ed. 36 (1997) 800–811.
[2] E.L. Zhou, P. Huang, C. Qin, K.Z. Shao, Z.M. Su, A stable luminescent anionic porous metal-organic framework for moderate adsorption of CO_2 and selective detection of nitro explosives, J. Mater. Chem. A 3 (2015) 7224–7228.
[3] C.D. Rickert, R. Beauchamp Jr., P. Cossum, in: D.R. Buhler, D.J. Reed (Eds.), Ethel Browning's Toxicity and Metabolism of Industrial Solvents, 2, Second Edition, Elsevier, Amsterdam, 1990, pp. 383–387.
[4] R.G. Ewing, D.A. Atkinson, G.A. Eiceman, G.J. Ewing, A critical review of ion mobility spectrometry for the detection of explosives and explosive related compounds, Talanta 54 (2001) 515–529.
[5] C.P. Chang, C.Y. Chao, J.H. Huang, A.K. Li, C.S. Hsu, M.S. Lin, B.R. Hsieh, A.C. Su, Fluorescent conjugated polymer films as TNT chemosensors, Synth. Met. 144 (2004) 297–301.
[6] Y. Zhang, X.X. Ma, S.C. Zhang, C.D. Yang, O.Y. Zheng, X.R. Zhang, Direct detection of explosives on solid surfaces by low temperature plasma desorption mass spectrometry, Analyst 134 (2009) 176–181.
[7] J.S. Caygill, S.D. Collyer, J.L. Holmes, F. Davis, S.P.J. Higson, Disposable screen-printed sensors for the electrochemical detection of TNT and DNT, Analyst 138 (2013) 346–352.
[8] N.D. Hoa, N.V. Duy, S.A. El-Safty, N.V. Hieu, Meso-/nanoporous semiconducting metal oxides for gas sensor applications, J. Nanomater. 2015 (2015) 1–14.
[9] S.T. Jean, Y.C. Her, Growth mechanism and photoluminescence properties of In_2O_3 nanotowers, Cryst. Growth Des. 5 (2010) 2104–2110.
[10] G.Z. Shen, B. Liang, X.F. Wang, H.T. Huang, D. Chen, Z.L. Wang, Ultrathin In_2O_3 nanowires with diameters below 4 nm: synthesis, reversible wettability switching behavior, and transparent thin-film transistor applications, ACS Nano 5 (2011) 6148–6155.

[11] A. Vomiero, S. Bianchi, E. Comini, G. Faglia, M. Ferroni, G. Sberveglieri, Controlled growth and sensing properties of In_2O_3 nanowires, Cryst. Growth Des. 7 (2007) 2500–2504.
[12] J.Q. Xu, Y.P. Chen, Q.Y. Pan, Q. Xiang, Z.X. Cheng, X.W. Dong, A new route for preparing corundum-type In_2O_3 nanorods used as gas-sensing materials, Nanotechnology 18 (2007) 1–7.
[13] S.G. Wang, P. Wang, Z.F. Li, C.H. Xiao, B.X. Xiao, R. Zhao, T.Y. Yang, M.Z. Zhang, Facile fabrication and enhanced gas sensing properties of In_2O_3 nanoparticles, New J. Chem. 38 (2014) 4879–4884.
[14] P. Li, H.Q. Fan, Porous In_2O_3 microstructures: hydrothermal synthesis and enhanced Cl_2 sensing performance, Mater. Sci. Semicond. Process. 29 (2015) 83–89.
[15] S.K. Lim, S.H. Hwang, D. Chang, S. Kim, Preparation of mesoporous In_2O_3 nanofibers by electrospinning and their application as a CO gas sensor, Sens. Actuators B: Chem. 149 (2010) 28–33.
[16] W.J. Kim, D. Pradhan, Y. Sohn, Fundamental nature and CO oxidation activities of indium oxide nanostructures: 1D-wires, 2D-plates, and 3D-cubes and donuts, J. Mater. Chem. A 1 (2013) 10193–10202.
[17] P. Li, H.Q. Fan, Y. Cai, In_2O_3/SnO_2 heterojunction microstructures: facile room temperature solid-state synthesis and enhanced Cl_2 sensing performance, Sens. Actuators B: Chem. 185 (2013) 110–116.
[18] Y.S. Li, J. Xu, J.F. Chao, D. Chen, S.X. Ouyang, J.H. Ye, G.Z. Shen, High-aspect-ratio single-crystalline porous In_2O_3 nanobelts with enhanced gas sensing properties, J. Mater. Chem. 21 (2011) 12853–12857.
[19] R.Q. Xing, Q.L. Li, L. Xia, J. Song, L. Xu, J.H. Zhang, Y. Xie, H.W. Song, Au-modified three-dimensional In_2O_3 inverse opals: synthesis and improved performance for acetone sensing toward diagnosis of diabetes, Nanoscale 7 (2015) 13051–13060.
[20] N. Singh, C.Y. Yan, P.S. Lee, Room temperature CO gas sensing using Zn-doped In_2O_3 single nanowire field effect transistors, Sens. Actuators B: Chem. 150 (2010) 19–24.
[21] N. Singh, R.K. Gupta, P.S. Lee, Gold-nanoparticle-functionalized In_2O_3 nanowires as CO gas sensors with a significant enhancement in response, ACS Appl. Mater. Interfaces 3 (2011) 2246–2252.
[22] P. Li, H.Q. Fan, Y. Cai, Mesoporous In_2O_3 structures: hydrothermal synthesis and enhanced Cl_2 sensing performance, Colloids Surf. A 453 (2014) 109–116.
[23] P. Li, H.Q. Fan, Y. Cai, M.M. Xu, Zn-doped In_2O_3 hollow spheres: mild solution reaction synthesis and enhanced Cl2 sensing performance, CrystEngComm 16 (2014) 2715–2722.
[24] S.J. Kim, I.S. Hwang, J.K. Choi, Y.C. Kang, J.H. Lee, Enhanced C_2H_5OH sensing characteristics of nano-porous In_2O_3 hollow spheres prepared by sucrose-mediated hydrothermal reaction, Sens. Actuators B: Chem. 155 (2011) 512–518.
[25] E. Li, Z.X. Cheng, J.Q. Xu, Q.Y. Pan, W.J. Yu, Y.L. Chu, Indium oxide with novel morphology: synthesis and application in C_2H_5OH gas sensing, Cryst. Growth Des. 9 (2009) 2146–2151.
[26] W.L. Zang, Y.X. Nie, D. Zhu, P. Deng, L.L. Xing, X.Y. Xue, Core–shell In_2O_3/ZnO nanoarray nanogenerator as a self-powered active gas sensor with high H_2S sensitivity and selectivity at room temperature, J. Phys. Chem. C 118 (2014) 9209–9216.
[27] L. Xu, B. Dong, Y. Wang, X. Bai, Q. Liu, H.W. Song, Electrospinning preparation and room temperature gas sensing properties of porous In_2O_3 nanotubes and nanowires, Sens. Actuators B: Chem. 147 (2010) 531–538.
[28] C. Li, D.H. Zhang, B. Lei, S. Han, X.L. Liu, C.W. Zhou, Surface treatment and doping dependence of In_2O_3 nanowires as ammonia sensors, J. Phys. Chem. B 107 (2003) 12451–12455.
[29] Q. Qi, P.P. Wang, J. Zhao, L.L. Feng, L.J. Zhou, R.F. Xuan, Y.P. Liu, G.D. Li, SnO_2 nanoparticle-coated In_2O_3 nanofibers with improved NH_3 sensing properties, Sens. Actuators B: Chem. 194 (2014) 440–446.
[30] L.J. Guo, X.P. Shen, G.X. Zhu, K.M. Chen, Preparation and gas-sensing performance of In_2O_3 porous nanoplatelets, Sens. Actuators B: Chem. 155 (2011) 752–758.
[31] J.Y. Liu, T. Luo, F.L. Meng, K. Qian, Y.T. Wan, J.H. Liu, Porous hierarchical In_2O_3 micro-/nanostructures: preparation, formation mechanism, and their application in gas sensors for noxious volatile organic compound detection, J. Phys. Chem. C 114 (2010) 4887–4894.
[32] J. Du, M. Yang, S.N. Cha, D. Rhen, M. Kang, D.J. Kang, Indium hydroxide and indium oxide nanospheres, nanoflowers, microcubes, and nanorods: synthesis and optical properties, Cryst. Growth Des. 8 (2008) 2312–2317.
[33] J. Zhao, Y.P. Liu, M.H. Fan, L. Yuan, X.X. Zou, From solid-state metal alkoxides to nanostructured oxides: a precursor-directed synthetic route to functional inorganic nanomaterials, Inorg. Chem. Front. 2 (2015) 198–212.
[34] E. Uchaker, N. Zhou, Y.W. Li, G.Z. Cao, Polyol-mediated solvothermal synthesis and electrochemical performance of nanostructured V_2O_5 hollow microspheres, J. Phys. Chem. C 117 (2013) 1621–1626.
[35] L.S. Zhong, J.S. Hu, H.P. Liang, A.M. Cao, W.G. Song, L.J. Wan, Self-assembled 3D flowerlike Iron Oxide nanostructures and their application in water treatment, Adv. Mater. 18 (2006) 2426–2431.
[36] J.J. Zhang, Y.L. Chen, Y.F. Sun, T. Huang, A.S. Yu, Hierarchical hollow Fe_2O_3 micro-flowers composed of porous nanosheets as high performance anodes for lithium-ion batteries, RSC Adv. 3 (2013) 20639–20646.
[37] G.H. Tian, Y.J. Chen, W. Zhou, K. Pan, C.G. Tian, X.R. Huang, H.G. Fu, 3D hierarchical flower-like TiO_2 nanostructure: morphology control and its photocatalytic property, CrystEngComm 13 (2011) 2994–3000.
[38] X. Zhou, X.W. Li, H.B. Sun, P. Sun, X.S. Liang, F.M. Liu, X.L. Hu, G.Y. Lu, Nanosheet-assembled $ZnFe_2O_4$ hollow microspheres for high-sensitive acetone sensor, ACS Appl. Mater. Interfaces 7 (2015) 15414–15421.
[39] X.M. Xu, X. Li, W.B. Wang, B. Wang, P. Sun, Y.F. Sun, G.Y. Lu, In_2O_3 nanoplates: preparation, characterization and gas sensing properties, RSC Adv. 4 (2014) 4831–4835.
[40] H.J. Kim, H.M. Jeong, T.H. Kim, J.H. Chung, Y.C. Kang, J.H. Lee, Enhanced ethanol sensing characteristics of In_2O_3-decorated NiO hollow nanostructures via modulation of hole accumulation layers, ACS Appl. Mater. Interfaces 6 (2014) 18197–18204.
[41] L.J. Zhou, Y.C. Zou, J. Zhao, P.P. Wang, L.L. Feng, L.W. Sun, D.J. Wang, G.D. Li, Facile synthesis of highly stable and porous Cu_2O/CuO cubes withenhanced gas sensing properties, Sens. Actuators B: Chem. 188 (2013) 533–539.
[42] H.F. Lu, F. Li, G. Liu, Z.G. Chen, D.W. Wang, H.T. Fang, G.Q. Lu, Z.H. Jiang, H.M. Cheng, Amorphous TiO_2 nanotube arrays for low-temperature oxygen sensors, Nanotechnology 19 (2008) 405504–405511.
[43] H.X. Yang, S.P. Wang, Y.Z. Yang, Zn-doped In_2O_3 nanostructures: preparation, structure and gas-sensing properties, CrystEngComm 14 (2012) 1135–1142.
[44] C.Q. Ge, C.S. Xie, S.Z. Cai, Preparation and gas-sensing properties of Ce-doped ZnO thin-film sensors by dip-coating, Mater. Sci. Eng. B 137 (2007) 53–58.
[45] N. Inamoto, S. Masuda, Revised method for calculation of group electronegativities, Chem. Lett. 100 (1982) 1003–1006.
[46] Z. Guo, J.Y. Liu, Y. Jia, X. Chen, F.L. Meng, M.Q. Li, J.H. Liu, Template synthesis, organic gas-sensing and optical properties of hollow and porous In_2O_3 nanospheres, Nanotechnology 19 (2008) 345704–345713.
[47] J.R. Sohn, Nitromethane sensing characteristics of SnO_2 gas sensors and infrared spectroscopic study, J. Ind. Eng. Chem. 8 (2002) 386–392.
[48] P.P. Jin, X.X. Zou, L.J. Zhou, J. Zhao, H. Chen, Y. Tian, G.D. Li, Biopolymer-assisted construction of porous SnO_2 microspheres with enhanced sensing properties, Sens. Actuators B: Chem. 204 (2014) 142–148.
[49] Z.H. Li, Y. Li, Y.X. Luan, J.C. Li, A.X. Song, $In(OH)_3$ particles from an ionic liquid precursor and their conversion to porous In_2O_3 particles for enhanced gas sensing properties, CrystEngComm 15 (2013) 1706–1714.
[50] S.J. Choi, M.P. Kim, S.J. Lee, B.J. Kim, I.D. Kim, Facile Au catalyst loading on the inner shell of hollow SnO_2 spheres using Au-decorated block copolymer sphere templates and their selective H_2S sensing characteristics, Nanoscale 6 (2014) 11898–11903.

Biographies

Yang-Yang He is a master student in State Key Laboratory of Inorganic Synthesis & Preparative Chemistry, Jilin University in China. She has majored in the synthesis of gas sensing nanomaterials.

Xu Zhao is a full professor in College of Chemistry, Jilin University (China). She received her M.Sc (1999) and Ph.D (2003) from Jilin University. Her research interest is the synthesis of nanomaterials and porous materials.

Yang Cao is a currently a Ph.D candidate in State Key Laboratory of Inorganic Synthesis & Preparative Chemistry, Jilin University in China. His research interest is the synthesis of sensing nanomaterials.

Xiaoxin Zou was awarded a Ph.D. in Inorganic Chemistry from Jilin University (China) in 06/2011; and then moved to the University of California, Riverside and Rutgers, The State University of New Jersey as a Postdoctoral Scholar from 07/2011 to 10/2013. He is currently an associate professor in Jilin University. His research interests focus on the design and synthesis of noble metal-free, nanostructured and/or nanoporous materials for water splitting, renewable energy applications and others.

Guo-Dong Li is a full professor at State Key Lab of Inorganic Synthesis & Preparative Chemistry, College of Chemistry, Jilin University in China. He received his B.Sc. (1995), M.Sc (1998) and Ph.D (2001) from Jilin University. His research interests include chemical sensors, lithium ion batteries and water splitting.